

BIT ERROR PREDICTION FOR DIGITAL IMAGE DATA

J. Q. Trelewicz and Douglas Cochran

Department of Electrical Engineering, Arizona State University, Tempe, Arizona 85287-7206

ABSTRACT

A nonideal two-dimensional optical system, as encountered in digital holographic data storage applications, can modify the intensity of transmitted digital data through beam shaping, focal surface distortion, and moiré patterns. Such changes in intensity can have significant adverse effects on digital data recovery at the receiver (e.g., a CCD camera). Current research seeks to detect and correct classes of such distortion so that recovery methods can be applied to the received data. This paper discusses methods used to predict the locations of bit errors in the recovered data. Prediction information may be used as weighting information in the recovery algorithm and in the design of channel codes. Furthermore, the higher the level of distortion that can be tolerated in the system, the lower the cost of the corresponding lenses, making the system more tractable for commercialization.

1. INTRODUCTION

Two-dimensional digital imaging may be used in optical computing and optical storage applications. The work presented in this paper was motivated by broader research involving digital holographic data storage systems. Such applications differ from many imaging processing situations in that the bit error rate (BER) (rather than perceptual quality, for example) is the crucial performance criterion. The digital imaging system may thus be viewed as a two-dimensional version of a conventional communications channel, presenting many of the same challenges in channel characterization and coding.

- In the digital imaging system, an image is projected on an appropriate “transmitter” (e.g., a spatial light modulator, or SLM), which utilizes a grid of pixels capable of discrete light intensity levels. The SLM typically contains non-transmitting (“dead”) regions between pixels.
- The image is illuminated with a light source; e.g., a laser. The laser beam carries the information through

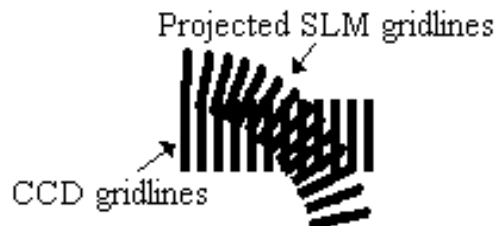


Figure 1: Theoretical structure of moiré patterns near the distortion region.

a series of elements that introduce noise and distortion: lenses, beam splitters, mirrors, and the like. These elements comprise the communications “channel.”

- The image is captured at a receiver, typically a Charge-Coupled Device (CCD) camera. The CCD pixels, like the SLM pixels, have a certain amount of dead space between. The result is that “sampling location” (i.e., the alignment between the SLM and the CCD pixels) is critical in data recovery. The captured image suffers from moiré fringes where the SLM and CCD pixels are ill-aligned. (Both the 1-to-1 pixel imaging and 1-to-4 pixel imaging systems analyzed suffer from these moiré fringes.) Figure 1 shows how the moiré fringes, which exist as the interference pattern between two regular grids, can be made to have a rounded shape near a high-distortion region where the projected SLM dead-region grid exhibits curvature.

Furthermore, since the intensity recorded by the CCD drops off as the square of distance from the focal surface, a non-planar focal surface can adversely affect the recorded image at the CCD.

For the purposes of this study, the main distinctions between the digital imaging system and the photographic imaging system are the presence of the moiré fringes and the non-smooth nature of the data. As noted above, imaging for storage or transmission of digital data differs from photographic imaging in the nature of performance criteria. Other crucial differences include the types of distortion encountered

E-mail: jentre@asu.edu. Experimental Data were obtained with the assistance of Optitek, Inc. All work was performed under NASA GSRP Fellowship NGT 5-22 through Goddard Space Flight Center.

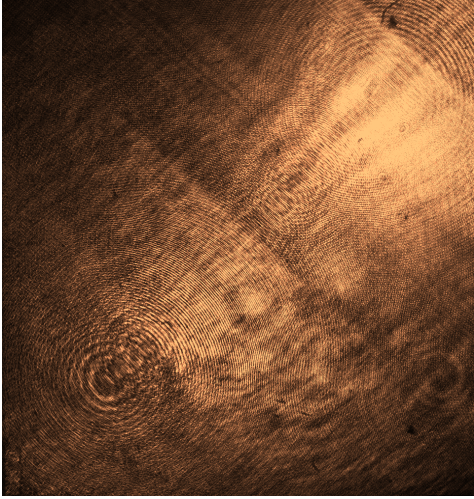


Figure 2: The image received at the CCD when a uniform image was “transmitted” by the SLM.

in digital storage and transmission applications, particularly the presence of strong moiré patterns and the statistical characteristics of the data itself.

This paper describes the nature of data distortion encountered in optical storage and transmission systems for digital data and presents a prototype algorithm for addressing one of the primary types of such distortion: the presence of moiré patterns.

2. SYSTEM DESCRIPTION

2.1. Channel

Distortion in the optical channel falls into several categories, including deterministic and random distortion. Figure 2 shows the result of transmitting a uniform image through the system. Many of the effects described below can be seen in this image.

Deterministic distortion includes shift-variant light intensity. Such variation is caused by several effects, including distortion from the lenses, finite aperture diffraction effects, back-reflections from the lenses, and source beam shaping.

These dominant effects may be described as follows:

- Finite aperture: This effect manifests itself as concentric rings in the image plane given by ([1])

$$\frac{I}{I_0} = \left(\frac{2J_1(\rho)}{\rho^2} \right)^2 \quad (1)$$

where R is the aperture radius, k is the wave number, $\rho = kR$, I_0 is the peak intensity, and J_1 is the Bessel function of the first kind. In the investigated systems,

as a result of the system design, only the Airy disk (the center bright ring) of the signal is seen in the image plane.

- Optical distortion: This effect includes spherical aberration, coma, astigmatism, and Petzval curvature effects. Optical distortion may be estimated by a polynomial in the object point height along the optical axis (parallel to the net direction of light propagation). ([2])
- Tilt: An object plane is imaged as a plane [3], allowing tilt in the system (from misalignment of mirrors and other elements) to be estimated in the image plane. Skew/tilt in the optical distortion and finite aperture results is assumed to be caused by tilt.
- Back reflection: Reflection occurs where the beam enters a lens. The reflected image traveling backward is reflected forward again by mirrors or other lenses in the system. Since a ray entering at an angle causes a reflection at that angle, the result may be a bright spot in the image plane, with a less bright reflected image appearing in a different portion of the image plane.

Because of the relatively large number of lenses in the investigated systems, finite aperture and optical distortion effects appear approximately Gaussian at the CCD, as suggested by the central limit theorem.

Random distortion in the channel includes dust and aberrations in the optical elements. Diffraction effects are seen at the locations of these objects. By duality, point objects cause patterns in the image plane in keeping with (1).

In the holographic data storage application, the storage medium may also contribute other channel effects. The data analyzed herein were imaged through a LiNbO_3 crystal, which does not appear to contribute significantly to the channel distortion.

2.2. Data Recovery

The data itself may be recovered from redundancy induced at the transmitter or from edge detail. The object of the authors’ current research is to apply correction for channel errors where possible and to estimate the location of data errors where correction is more challenging. The estimation of the focal surface allows several gains to be made in processing of the received signal. Firstly, the point spread function (PSF) can be estimated, allowing some correction of blurring to be made. Also, the location of moiré patterns can be estimated, facilitating the use of “confidence weights” during data decoding.

Because of the shift-variance and nonlinearity of the channel, the investigated systems are significantly more complicated than the LSI systems investigated by [4] and others

who estimate the PSF from edge and from windowed detail. The work of [3] suggests methods for recovering the focal surface through the analysis of multiple system images at different focal lengths. The system under evaluation in this study allows only one focal image of each data set to be recorded, limiting the applicability of such approaches. Once the intensity variation is estimated and corrected in the image, methods such as those suggested by [5] can be used to recover bilevel data by detecting edge detail.

Since moiré patterns create false edges in the image plane, they can raise the BER significantly if edge detection or thresholding methods are used in data recovery.

3. ANALYSIS OF EXPERIMENTAL DATA

The data analyzed in this study were obtained from several optical systems with similar arrangement but with separate alignment. The input data were imaged on reflective 8-bit grayscale SLMs and recorded with the use of 8-bit grayscale CCD cameras.

The experimental data exhibit roughly two classes of focal surface error: Gaussian surface (from optical distortion) and planar tilt. Data from the Gaussian surface class were evaluated for this study, since tilt can be corrected through optical alignment. The Gaussian surface test data included bilevel random “bits” (white or black pixels), filled between 10% and 50%. The system was manually aligned for all data sets. One third of the test data exhibited “best” alignment and focus, one third suffered from focus errors, and the remaining third showed magnification errors.

Analyzed empirical data show that the fringes are most prominent near the inflection points of the Gaussian. (The fringes appear approximately where the first derivative has the highest fourth of its magnitude.) This matches with theory, since the maximum distortion of the grid occurs in this region. Figure 3 shows the actual moiré fringes in this region (compare with figure 1). Figure 4 shows the expected fringe locations for a simulated grid.

3.1. Algorithm Description

The shape of the focal plane is estimated from the shape of the primary beam and its back reflections. This shape information is then used to estimate the locations of the moiré patterns. If the primary spot is centered perfectly on the distortion, the spot will be distorted with circular symmetry. Thus, the system may be aligned with the primary spot deliberately off-center so that shaping of the spot occurs.

First, a median filter is passed over the CCD image to remove the bit data. The location of the primary beam spot is estimated by its intensity near the brightest area in the filtered data. More sophisticated methods, such as those



Figure 3: A distorted region of an actual received data image. Some moiré fringes are highlighted with arrows.

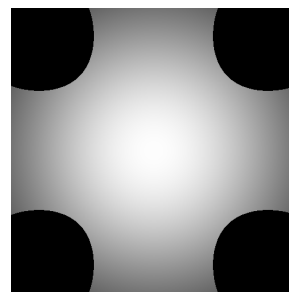


Figure 4: Dark regions show the expected location of fringes for $\sigma = 200$ on a 500×500 grid.

outlined in [6], may be used in future work to locate the primary and reflected beam spots in the image field.

The shape of the primary spot is used to estimate the center of the distortion Gaussian and its standard deviation. Figure 5 shows the relation between the spot shape and the parameters of the distortion. The center of the distortion can be approximated from rays drawn normal to the lines tangent to the circle along which d_2 is measured. Because system alignment approximately centers the optical elements in the optical path, the distortion Gaussian is assumed to be nearly centered on the CCD, thereby reducing the error introduced by the estimation.

The standard deviation of the distortion is estimated as follows: put d the spot diameter, where the spot intensity has dropped to about 50% of its peak intensity. (This value was chosen to attempt separation of the primary and the reflected spots.) Put p_1 and p_2 the points at which the spot is tangent to the circles, as shown in figure 5. Then $d_1 = |p_1 - p_2|$. Note that

$$d_2 \approx d = \int_C e^{-x^2/2\sigma^2} dx$$

where C is the contour running from p_2 to p_1 on the distortion surface.

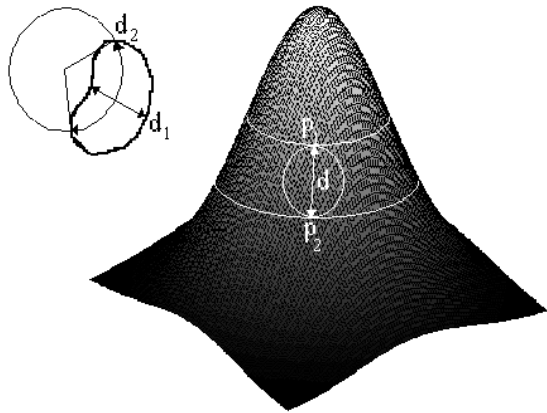


Figure 5: Distortion parameter estimation from spot shape.

3.2. Analysis Results

Using the simulated grid as in figure 4, the estimated σ for the experimental data is roughly 150.

Because the algorithm uses intensity reduction to locate the primary spot, mis-estimation of the spot shape may occur if the primary and the reflected spots are very close. It is anticipated that an algorithm that employs intelligence to locate the multiple spots may be able to overcome this problem in future work.

The algorithm located the primary spot without problems, but some bleed from the reflected spots still caused problems with finding the dimensions of the spot. Therefore, the algorithm was run with assistance (the reflected spots were identified manually). Because of uncertainty in the exact curvature of the primary spot, σ could only be estimated to within an order of magnitude. However, d_2/d_1 correlated well to the first derivative of the Gaussian: $d_2/d_1 \approx 2.6$ near the inflection point, with smaller values near the center. Using the inflection point, σ was estimated with 20-30% error when the center of the spot was used, and with less than 15% error when the inside edge of the spot was used.

3.3. Discussion

The closeness of the primary and the reflected spots requires the use of an algorithm that can locate and separate the points. Because the tested algorithm does not employ this strategy, some of the images result in too-large estimates of d_1 , inhibiting the ability of the algorithm to estimate the distortion parameters.

In those cases in which the spots were not too close together for spot location estimation, σ could be estimated by comparing d_2/d_1 for several images where the primary

spot was moved from the center of the image toward the edge. This method could be used with a single image if the reflected spots were also located, since the primary and reflected spots could be arranged to cover the image region from near-center to edge.

Continuing study will employ more sophisticated algorithms for locating the spots. It is anticipated that more accurate estimates for σ will be obtained with that data.

4. CONCLUSIONS AND FUTURE WORK

The digital imaging system resembles the conventional communications channel in many ways. However, additional challenges are posed by the three-dimensional nature of the optical channel. Current results on estimating the location of moiré fringes, leading to possible bit errors, are discussed.

The prototype algorithm presented in this paper relies on relationships between the parameters d_1 and d_2 which are unlikely to hold in a broad class of actual systems. Thus, further work will be needed to develop an approach sufficiently robust to be of significant practical value in the prediction of the bit error distribution and in the design of codes. Nonetheless, this first look at the problem provides insight into properties of an optical system that may be critical in developing more practical algorithms.

5. REFERENCES

- [1] G. R. Fowles, *Introduction to Modern Optics*. New York: Holt, Rinehart, and Winston, Inc., 1975.
- [2] *US Dept. of Defense MIL-HDBK-141: Optical Design*. Washington, DC: Defense Supply Agency, 1962.
- [3] M. Subbarao and T. Choi, "Accurate recovery of three-dimensional shape from image focus," *IEEE Transactions on Pattern Analysis and Machine Intelligence*, vol. 17, p. 266, March 1995.
- [4] B. Chalmond, "PSF estimation for image deblurring," *CVGIP. Graphical Models and Image Processing*, vol. 53, p. 364, July 1991.
- [5] R. Joseph and T. Pavlidis, "Deblurring of bilevel waveforms," *IEEE Transactions on Image Processing*, vol. 2, p. 223, April 1993.
- [6] R. N. Strickland and H. I. Hahn, "Wavelet transform methods for object detection and recovery," *IEEE Transactions on Image Processing*, vol. 6, p. 724, May 1997.